Real-Time Motion Correction in 2D Multi-Slice Imaging with Through-Plane Navigator

Wei Lin[1], Tim Nielsen[2], Qin Qin[3,4], Stewart H Mostofsky[5,6], and Randy Duensing[1]

[1]Invivo Corporation, Philips Healthcare, Gainesville, Florida, United States, [2]Philips Research Europe, Hamburg, Germany, [3]Radiology, The Johns Hopkins University, Baltimore, Maryland, United States, [4]F.M. Kirby Research Center, Kennedy Krieger Institute, Baltimore, Maryland, United States, [5]Neurology and Psychiatry, The Johns Hopkins University, Baltimore, Maryland, United States, [6]Kennedy Krieger Institute, Baltimore, Maryland, United States

Introduction

Imaging artifact caused by through-plane bulk subject motion remains an unmet challenge in 2D multi-slice multi-shot MR imaging sequences, which are current clinical workhorses. Through-plane motion disrupts the consistency of the imaging volume and therefore needs to be corrected prospectively. Retrospective methods such as PROPELLER [1] can only reject partial data corrupted by through-plane motion, which is insufficient unless subject returns to the same position. Existing prospective motion correction techniques require either marker(s) to be attached to the subject [2-3] or additional navigators [4-5]. Markers increase patient discomfort and introduce additional workflow delays. All existing prospective navigators use additional 3D excitations, which are susceptible to interference from 2D slice-selective imaging excitations. In this work, a prospective through-plane navigator (tNav) strategy is proposed without introducing any additional RF excitation. When combined with a prospective orbital navigator (oNav), 3D rotation/translation (six degrees of freedom) is detected and corrected in real time.

Methods

The proposed tNav strategy samples the $k_x = 0$ and the $k_y = 0$ lines in the k-space for each 2D imaging slice (Fig. 1a-1b), where x and y are readout and phase-encode directions, respectively. After an inverse Fourier Transform (FT) is applied along k_x/k_y direction, tNav data from all coil elements and slices are combined to reconstruct two mutually orthogonal tNav projection images, both orthogonal to the imaging slices (Fig. 1c). These images are used to detect two through-plane rotation and three translation parameters in real-time using an image correlation measure, which is robust against unaccounted rotation orthogonal to each tNav image plane and noise. The remaining rotation within the imaging plane is detected by replacing tNav with an orbital navigator [6] on the last slice. Motion parameters are then used to update RF frequency, gradient waveform and receiver frequency/phase in the next TR and compensate for the effect of motion. Motion-corrupted TRs are rejected and re-acquired.

Two healthy volunteers were scanned on a clinical 3.0T scanner (Achieva, Philips, the Netherlands) using an 8-channel head coil (Invivo, Gainesville). A 2D multi-slice turbo spin-echo (TSE) sequence was modified to allow the proposed real-time motion correction method with following parameters: FOV 230×230 mm^2, slice thickness 5mm, matrix size 256 (readout) × 256 (view no.), TR/TE = 6 sec / 80 ms, echo train length = 16, total scan time 1.5 minute. The first experiment validates the accuracy of motion detection. Two motion-free scans in the same orientation were separated by a motion-corrupted scan in an orthogonal plane, during which subject makes a mid-way through-plane rotation. The second experiment examines the overall efficacy of the proposed real-time motion correction scheme. Coronal and axial scans were performed, and volunteers were asked to perform both nodding ("YES") and shaking ("NO") head motion during scans with real-time motion correction either turned on or off. Motion-free reference images were also acquired for comparison.

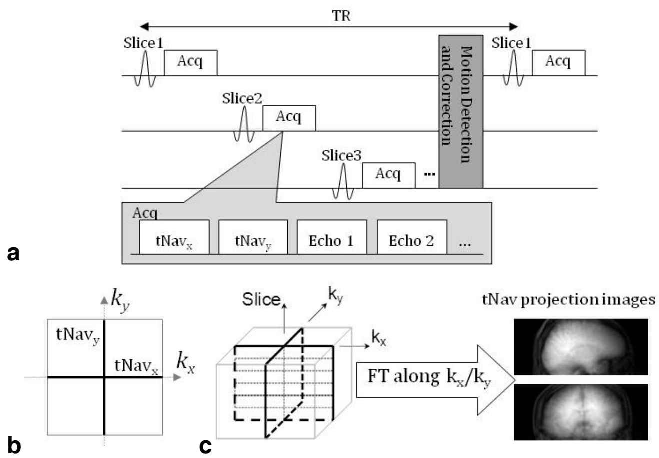

Figure 1 The scheme of tNav. **(a)** Two tNav echoes are inserted into the acquisition window of each slice. Real-time motion detection and correction is carried out at the end of each TR. **(b)** Two tNav echoes sample the k-space of each slice along the $k_x = 0$ and the $k_y = 0$ lines. **(c)** After an inverse FT is taken along k_x/k_y direction, two orthogonal tNav projection images are reconstructed for through-plane motion detection.

Results and Discussions

Figure 2 shows images from a validation experiment. Axial images (Fig. 2a) acquired before and after the motion-corrupted coronal scan are consistent with tNav images acquired during the coronal scan before and after motion occurred. Rotations detected from correlation of tNav images and from registration of axial images were both 16.0^o.

Figure 3 shows results from a motion correction experiment. Motion introduces severe ghosting artifacts (Fig. 3b). When real-time motion correction with tNav/oNav was enabled, image quality was dramatically improved (Fig. 3c), similar to motion-free scan (Fig. 3a). The maximal 3D rotation detected from tNav/oNav data was (0.3^o, -0.7^o, 3.8^o), which is dominated by through-plane rotation around the head-foot axis.

The proposed method can be applied to any 2D multi-slice multi-shot sequences by inserting tNav/oNav echoes and real-time motion detection and correction module. For multi-shot diffusion sequences, tNav can also be used to correct additional phase error accumulated during the diffusion-sensitizing gradient.

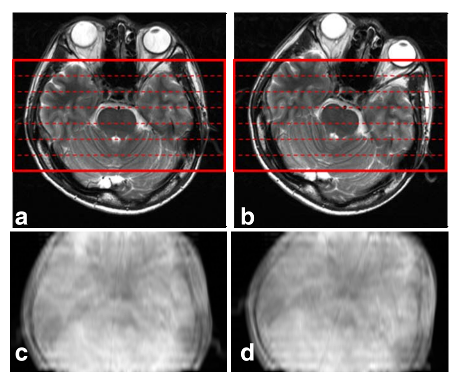

Figure 2 Validation of motion detection with tNav. **(a) – (b)** Axial images acquired before and after a motion-corrupted coronal scan. **(c) – (d)** tNav images acquired before and after motion occurred during the coronal scan.

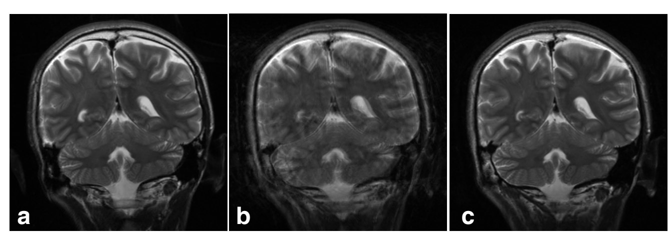

Figure 3 In vivo motion correction results in a multi-slice coronal scan. **(a)** Motion-free scan. **(b)** Motion-corrupted scan. **(c)** Motion-corrupted scan with real-time tNav/oNav motion correction enabled.

References

[1] Pipe JG. *MRM* 1999; 42: 963-969.
[2] Zaitsev M, et al. *Neuroimage* 2006; 31: 1038-1050.
[3] Ooi MB, et al. *MRM* 2009; 62: 943-954.
[4] Van der Kouwe AJW, et al. *MRM* 2006; 56: 1019-1032.
[5] White N, et al. *MRM* 2010; 63: 339-348.
[6] Fu ZW, et al. *MRM* 1995; 34: 746-753.